Polyacrylonitrile/Ag Nanoparticles Nanofibers as an Efficient Adsorbent for Natural Gas Condensate Desulfurization

Dadashvand Nigjeh, Reza; Alimoradi, Mohammad*[+]

Department of Chemistry, Faculty of Science, Arak Branch, Islamic Azad University, Arak, I.R. IRAN

Mollahosseini, Afsaneh*[+]

Faculty of Chemistry, Iran University of Science and Technology, Tehran, I.R. IRAN

Remezani, Majid

Faculty of Science, Department of Chemistry, Arak Branch, Islamic Azad University, Arak, I.R. IRAN

ABSTRACT: *In this work, the optimization of the synthesis of PAN/Ag nanofiber composites via electrospinning was investigated via Taguchi's experimental design approach. The adsorption capacity of sulfur compounds from natural gas condensate was considered an objective function. The PAN/Ag nanofiber with 11 wt% PAN, 45 wt% $AgNO_3$, 15 kV applied voltage, and 15 cm for a distance of a needle to a collector showed the highest adsorption capacity. The SEM, EDX, TEM, XRD, and FT-IR techniques were employed to elucidate the optimized PAN/Ag nanofiber structure. The results showed the successful synthesis of PAN/Ag nanofibers with diameters in 100-300 nm range and well distribution of Ag nanoparticles in the polymeric matrix. In addition, optimization of the adsorption capacity of PAN/Ag nanofiber in desulfurization of natural gas condensate in batch mode was performed via central composite design. Four factors including adsorbent weight, sulfur concentration in the natural gas condensate, the volume of the sample, and the adsorption time were considered effective factors each in three levels. The ANOVA analysis showed the more important factor in adsorbent performance is the concentration of sulfur in gas condensate and the weight of the adsorbent. The interaction terms between time and concentration and between volume and concentration are also important in response. Moreover, the response surface analysis of interaction terms showed the adsorptive nature of desulfurization.*

KEYWORDS: *Desulfurization; Electrospinning; Reactive adsorption; Polyacrylonitrile; Experimental design.*

INTRODUCTION

Organic sulfur compounds are the main pollutant of natural gas condensates. These compounds are considered as a primary source of air pollution because their burning products are caused by acid rain. Moreover, the corrosion

* *To whom correspondence should be addressed.*
+ E-mail: m-alimoradi@iau-arak.ac.ir , amollahosseini@iust.ac.ir
1021-9986/2022/5/1538-1548 11/$/6.01

nature of sulfur compounds causes destructive effects on downside equipment. In addition, the utility of sulfur-containing fuels in catalytic processes is also limited due to the poisonous nature of sulfur on heterogeneous catalysts; thus, the desulfurization of diesel and gasoline fuels, as well as gas condensates, has attracted the attention of many researchers [1].

To date, many desulfurization approaches have been reported. Among them, hydrodesulfurization (HDS) is the most widely used technology for the desulfurization of diesel fuel, which is highly effective for removing aliphatic and acyclic sulfur compounds (thiols, sulfides, and disulfides). In this process, hydrogen gas is used to remove sulfur compounds which yield hydrocarbons and H_2S. Due to a large amount of hydrogen consumption, high operational temperatures (> 300 °C), high pressures (3–10 MPa), and larger reactor volumes, several alternate desulfurization processes have been employed [2]. These approaches involve adsorption [3], extraction [4], oxidative desulfurization (ODS) [5], and biodesulfurization [6,7]. Compared to other technologies, the adsorptive removal of sulfur compounds is one of the promising approaches due to its easy operation conditions and its capability to remove sulfur at very low levels.

The adsorption technique has been regarded as a promising method for not only sulfur compound adsorption but also for a variable number of other compounds including dyes, pharmaceuticals, etc [8–10]. In this process, normally a porous and functionalized surface, known as an adsorbent, is used to remove impurities and pollutants (adsorbate) [11]. The efficiency of the whole process is determined by the interaction between adsorbent and adsorbent. Accordingly, the adsorption process is categorized into physical adsorption and chemical adsorption [12,13]. In order to reach the maximum performance of the adsorption process, it is important to investigate parameters, including time, initial concentration, and adsorbent dosage [14,15]. Common materials for the adsorptive removal of sulfur are zeolites, activated carbon, and alumina, which are porous materials and perform desulfurization mainly *via* physisorption. The modification of these adsorbents by transition metal ions results in reactive adsorption *via* σ–π bonds between metal ions and adsorbates and further enhanced their performance [16,17]. Optimization of sulfur adsorption over Ag-zeolite nano adsorbent has been reported by *Bakhtiari et al* [18]. They reached a thiophene adsorption efficiency close to 50 ppm, at 83 ˚C for adsorption temperature, 5.53 % for metal percent, and 436 ˚C for calcination temperature. In other work, the combination of electrochemical oxidation and solvent extraction was proposed to reduce the sulfur content in condensate gasoline. The sulfur content decreased from 3478.4 μg/g to 13.1 μg/g and the desulfurization efficiency reached 99.62% [19]. In another study, the desulfurization of liquid-fuel was done by $FeCl_3$-based deep eutectic solvents and optimized by central composite design [20]. Other research revealed that the Cu(I)Y zeolite, CuCl/MCM-41 are the most promising sorbents for natural gas desulfurization [21]. Studies ~~which~~ carried out by *Behl et al.* [22] revealed that Zn–Ti–O-based adsorbents with nanofibrous morphology can sustain their initial reactivity and sulfur removal capacity over multiple regeneration cycles.

Recently, it has been reported that the polystyrene nanofibrous membrane, prepared by electrospinning, and loaded with Ag^+ cations has the ability to be employed for deep desulfurization [23]. Electrospinning is a fascinating approach to the synthesis of nano-to-micro range fibers with well-defined diameters and morphologies [24]. In another work, Desulfurization of gasoline was done by using acrylonitrile electro-spun nanofibers and lead nanoparticles [25]. Due to the lack of studies in this area, the preparation conditions of polyacrylonitrile/Ag nanoparticles nanofibers *via* the Taguchi experimental design approach and the optimized nanofiber that was used for desulfurization of the natural gas condensate were investigated. In-situ reduction of Ag^+ ions by dimethylformamide as a solvent was used to prepare PAN-doped Ag nanoparticles. The results revealed the superior adsorption capacity of the synthesized nanofibers compared to the previously reported absorbents. Moreover, some characterization experiments were conducted to represent the structure of synthesized nanofibers and possible sulfur adsorption mechanisms.

EXPERIMENTAL SECTION

Materials

The PAN powder (150000 g/mol), dimethylformamide (DMF, 73.09 g/mol), $AgNO_3$ (the average size of silver nanoparticles is 20 – 80 nm), and all other materials were received from Aldrich and were used without further purification.

PAN/Ag nanofibers fabrication

PAN solution with different weight percentages was prepared by dissolving the appropriate amounts of PAN powder in DMF solvent under 2 h stirring, based on Eq. (1).

$$\mathrm{PAN}(\mathrm{wt.\%}) = \frac{m_{PAN(g)}}{m_{PAN(g)} + m_{DMF(g)}} \times 100 \quad (1)$$

After the preparation of PAN solution, the required amounts of $AgNO_3$ were added to it to obtain different weight percentages of Ag in nanocomposite as described in Eq. (2). This mixture was further left under stirring for 24 h.

$$AgNO_3(\mathrm{wt.\%}) = \frac{m_{AgNO_3(g)}}{m_{AgNO_3(g)} + m_{PAN(g)}} \times 100 \quad (2)$$

For electrospinning, PAN solution containing Ag nanoparticles was loaded in a 5 mL syringe with a stainless steel needle with 1 mm diameter attached to it. The syringe was attached to a syringe pump (KDS 200, KD Scientific Inc., MA) with the needle tip connected to a high voltage power supply (ES30P, Gamma High Voltage, FL). An aluminum sheet (20×20 cm) was used as a collector. The infusion rate was set to 1.5 mL/h. To optimize the conditions, the L9 orthogonal array of Taguchi experimental design approach with 4 factors each in 3 levels were employed. The factors and respective level values are given in Table 1. Minitab 16 software was used for Taguchi design.

Desulfurization tests

To evaluate the desulfurization efficiency of the prepared composite nanofibers, the adsorption capacity was calculated as described in Eq. (3)

$$\text{Adsorption capacity}(\mathrm{A.C}) = \frac{(C_0 - C) \times V}{m_{adsorbent}} \quad (3)$$

Where the *A.C.* is the adsorption capacity of nanocomposite in mg S/g adsorbent, C_0 and C are the initial and final concentration of sulfur in gas condensate in *mg/L*, *V* is the volume of specimen in *L*, and *m* depicts the mass of nanocomposite in *g*, as adsorbent.

To optimize the effect of synthesis conditions of PAN/Ag nanofibers on adsorption desulfurization, each specimen was subjected to 5 mL of gas condensate containing 100 ppm sulfur. After 10 min stirring, the remained sulfur of each solution was measured by a Total sulfur analyzer (TS3000, Thermo).

The Design Expert 7.0.0 software was used to optimize the operational conditions of desulfurization process.

Characterization

The morphology and the composition of PAN/Ag composite NFs were acquired by a field-emission scanning electron microscopy (FE-SEM MIRA3 FEG-SEM, Tescan, Czech) with an energy dispersive X-ray spectrometer (EDAX) (Genesis, XM2). The surface of the samples was coated with Au for 30 s prior to imaging. Transmittance electron microscope (TEM) photographs of the samples were examined by a Philips Tecnai F20 (Oregon, USA). The crystalline phases and the crystal structures of prepared NFs were investigated by X-Ray diffraction (XRD) spectra over a 2θ range from 10˚ to 70˚ on Siemens D-500 Diffractometer using Cu K_α radiation (wavelength, λ=1.5406 ˚A). Fourier Transform Infrared Spectroscopy (FT-IR) of the samples was recorded on Bruker Optics TENSOR 27 spectrometer using KBr pellets. To measure the sulfur content of gas condensates, a total sulfur analyzer was employed.

RESULTS AND DISCUSSION

Optimization of synthesis conditions of PAN/Ag nanofibers

Taguchi's experimental design approach was employed to optimize the synthesis conditions of PAN/Ag nanofibers. For this means, four factors including PAN wt%, $AgNO_3$ wt%, applied voltage (in kV), and the distance of needle tip to the collector (in cm) were considered as variables each in three levels and the injection flowrate was set to 1.5 mL/h. For a situation in which the large S/N ratio is better. The results are given in the last column in Table 1.

As seen, a maximum adsorption capacity of 33.3 ($mg._S/g_{\ Abs.}$) was obtained in run number 6. On the other hand, based on the main effects of factors depicted in Fig. 1, the optimum values of factors are 11 wt% PAN, 45 wt% $AgNO_3$, 15 kV applied voltage, and 15 cm for the distance of the needle to the collector. For two factors, the weight percentage of PAN and working voltage, the effects of factors on nanofiber performance are curve-shaped and the optimum values are in the employed range. In the case of applied voltage, it is well-known that values higher than the threshold

Table 1: Experimental ranges and levels in Taguchi experimental design for synthesis of PAN/Ag composite fibers.

Run number	PAN (wt.%)	$AgNO_3$ (wt.%)	Voltage (KV)	Distance (cm)	Adsorption capacity (mg S/g Abs.)
1	9	25	10	15	13.1
2	9	35	15	20	18.1
3	9	45	20	25	12.6
4	11	25	15	25	30.9
5	11	35	20	25	25
6	11	45	10	20	33.3
7	13	25	20	20	12.5
8	13	35	10	25	16.6
9	13	45	15	15	32.3

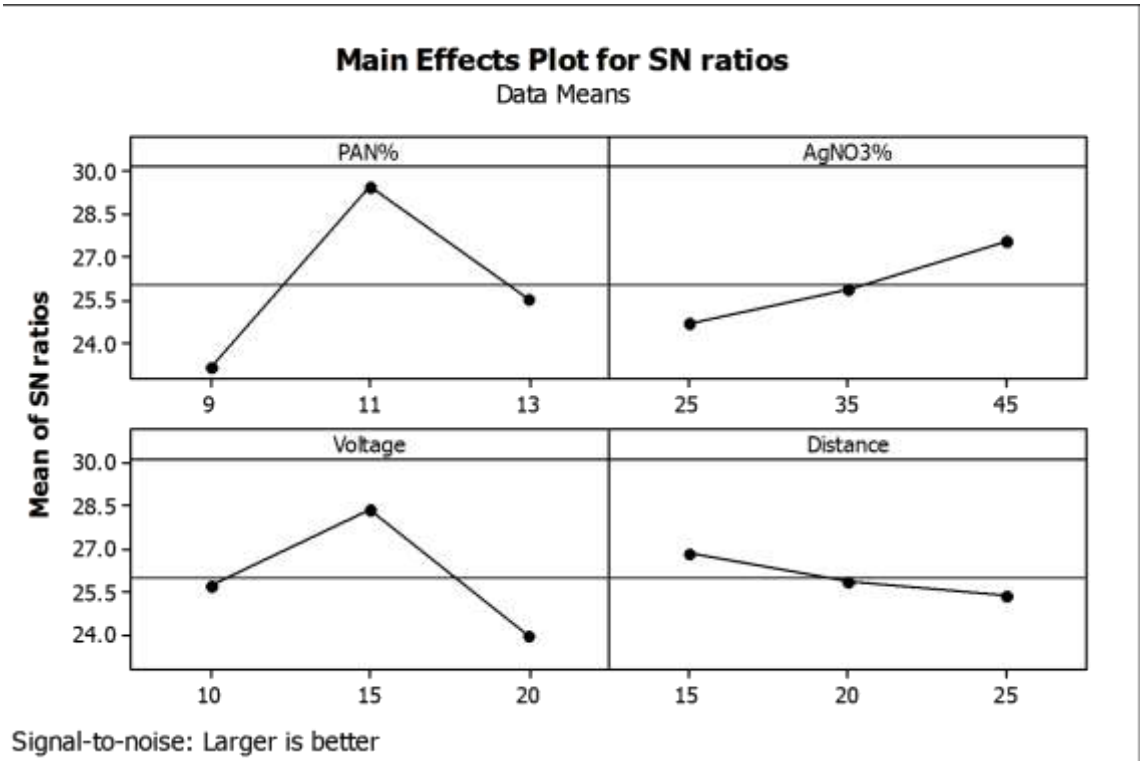

Fig. 1: Main effects plot for S/N ratios.

voltage, charged jets ejected from Taylor Cone can occur but the high values of working voltage offer a greater probability of beads formation and result in non-uniform fibers. On the other hand, the low working voltage results in fibers with higher diameters and thus less active surface area [23,26].

As a result, both in high and low voltages, the performances of fibers decreased. In the case of $AgNO_3$ wt%, an increasing trend was observed depicting its desired effect on sulfur removal. But due to the increase of two factors, PAN and $AgNO_3$ weight percentages, the viscosity of the solution was enhanced which resulted in the thickening of the nanofibers. Also, the increase of $AgNO_3$ wt% caused weak fiber formation. For the distance of the needle to the collector, a downward trend was observed. This factor had a direct effect on the flight time of injected

solution and thus on its drying time. This means that by increasing the distance, the fibers had more time to dry and vice versa; thus, 20 cm is sufficient enough to reach suitable fibers. It is respected that at low distances, such as 15 cm, the excess solution caused the conjugation of fibers in contacted regions and resulted in more strength-beaded fibers [23].

Structural characterization of optimum PAN/Ag nanofiber

Here some characterization techniques were employed to elucidate the structural features of the optimum sulfur adsorbent. As can be seen in Fig. 2, the SEM image of optimum PAN/Ag nanofibers shows uniform structures which piled up on each other, without beads-on-a-string morphology, owing to the good electrospinning ability of the core PAN solutions and the employed optimum conditions for electrospinning. The distribution of the nanofibers` diameters was also calculated from the SEM image and the results were depicted in Fig. 2 (b). As seen, the diameters of nanofibers were mainly in the the100-300 nm range. Moreover, the elemental analysis by EDX (Fig.2 (c)) represents the presence of C, N, O, and Ag atoms in the sample with 56.1 wt% and 12.9 atomic% from Ag indicating good loading of Ag nanoparticles into nanofibers. To have a better understanding of Ag distribution through the nanofibers, the elemental mapping of Ag was performed. As seen in Fig 2(c), the dotted image of mapping depicts the well-distribution of Ag in the texture of nanofibers, a situation that is necessary for reactive adsorption and removal of sulfur compounds from the solution. In addition, the TEM images of the PAN/Ag nanofibers show the distribution of black spots throughout the nanofibers with diameters less than 20 nm, which is attributed to the Ag nanoparticles. Moreover, the conjugation of nanofibers in some regions was also observed. This phenomenon increases the strength of nanofibers and boosts their application for membrane processes. As stated in 3.1, the distance of the needle to the collector is a critical factor in the drying process of electrospinning fibers, in which, under the defined conditions in this work the drying is not complete and thus causes the conjugation of fibers to each other to yield an entanglement network of PAN/Ag fibers.

To further understand the phase formation and the crystallinity of the sample, the powder XRD analysis was performed. The pattern, represented in Fig. 3 (a), clearly shows the characteristic peak attributed to PAN at 2θ's of 17. The peaks observed at 2θ's of 38, 45, 65.5, and 78.5 were attributed to the Ag planes of (111), (200), (220), and (311), respectively; thus, the XRD pattern proves the successful formation of two phases in the nanocomposite.

In-situ reduction of Ag+ ions in the presence of PAN by DMF as solvent and reductant was used to prepare PAN/Ag composite fibers [27–29], which follows a mechanism that involves the formation of carbamic acid. The color changed after the addition of Ag precursor to the PAN/DMF solution, from initially white to yellow then brown represented clearly the formation of Ag nanoparticles. Although the previous studies emphasized the formation of stable dispersion of Ag nanoparticles in the presence of 3-aminopropyltrimethoxysilane in this case, it is expected that the polymer network itself works as a stabilizer for the prepared nanoparticles. This opinion was further supported by TEM images as depicted in Fig. 2(e) and (f). Moreover, the carbamic acid decomposes somewhat to CO_2 and dimethylamine. The formed amine could be reduced by the cyanide groups of the polymer chain. Thus it is necessary to explore the functional groups of PAN and PAN/Ag fibers. For this means, the FT-IR spectra of PAN fibers and PAN/Ag fibers were taken. The spectrum of PAN, Fig. 3(b), shows peaks located at 2240 and 1250 cm^{-1} which is attributed to the stretching vibrations of cyanide groups in PAN, however, their intensity was significantly reduced for PAN/Ag fibers (Fig. 3(c)), indicating the reduction in the number of cyanide groups in polymer chains [28]. On the other hand, the appearance of a peak at 1665 cm^{-1} in PAN/Ag depicted the formation of C=N bonds. Also, a peak that appeared at 1100 cm^{-1} indicated the presence of C-N bonds related to dimethylamine in the matrix of the polymer. The wide peak around 2935 cm^{-1} is attributed to the stretching vibrations of C-H groups [30]. Therefore, the FT-IR spectra, as well as TEM images, approved the formation of Ag nanoparticles in the matrix of PAN.

Optimization of operation conditions for desulfurization of natural gas condensate by PAN/Ag nanofibers

After obtaining optimum PAN/Ag nanofibers and characterization of its structure, to reach optimum operating conditions for the removal of sulfur from natural gas condensates, a Central Composite Design (CCD) face center approach was employed. Four factors including

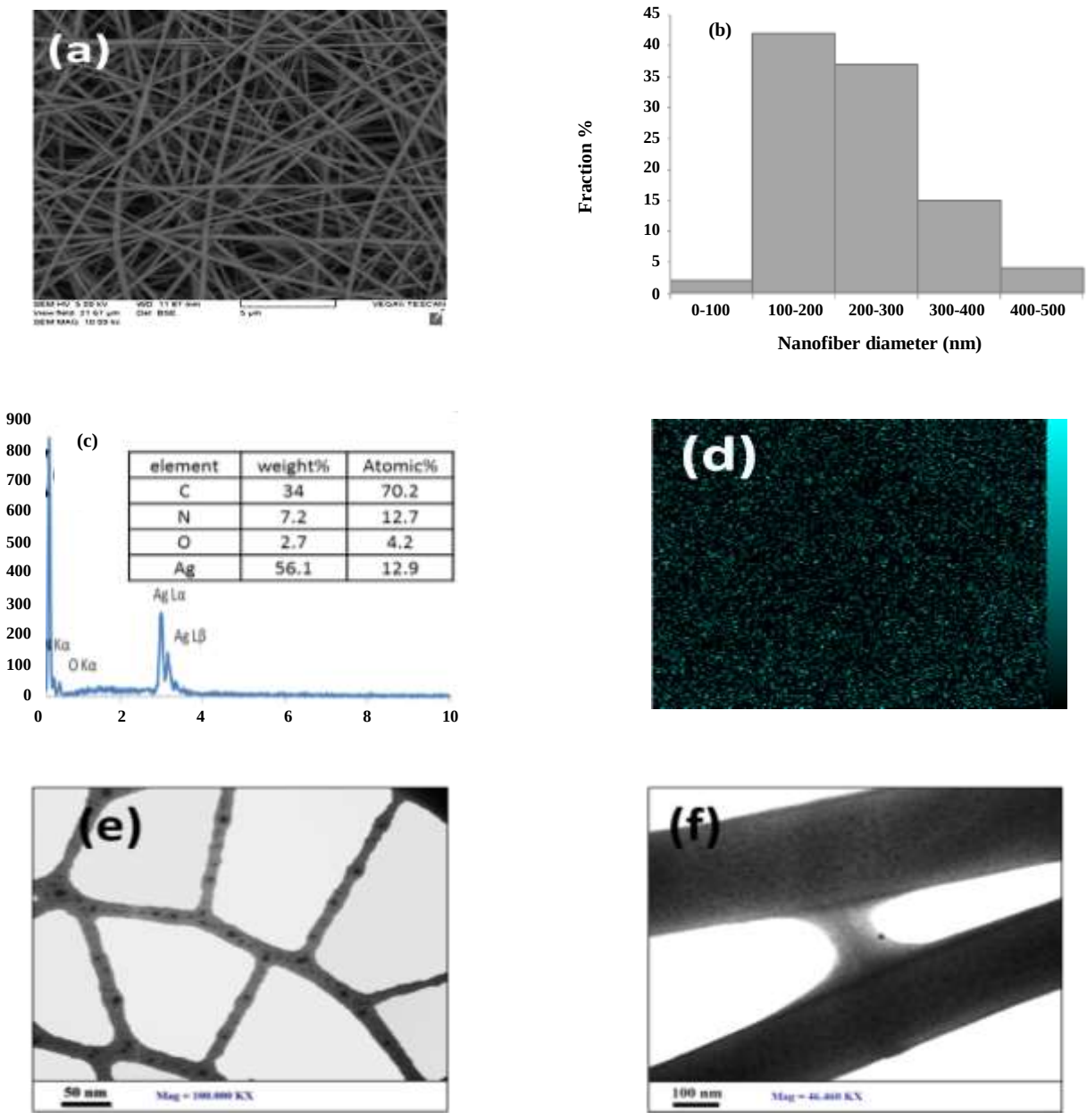

Fig. 2: (a) SEM image for PAN/Ag nanofiber, (b) Size distribution graph of the PAN/Ag nanofibers diameters, (c) EDX spectrum, (d) elemental mapping of Ag, and (e) and (f) TEM images of the PAN/Ag nanofibers.

adsorbent weight, sulfur concentration in the natural gas condensate, the volume of the sample, and the adsorption time were considered effective factors each in three levels as depicted in Table 2.

The conditions of each run and respective adsorption capacity are given in Table 3. The experiments have been carried out under similar environmental conditions, with relative humidity below 30% and a temperature of 25 ± 0.5 °C.

As Table 4 represents the first step, an analysis of variance was carried out to evaluate the response of experiments. The ANOVA analysis shows that among the four studied variables, the more significant factors in order are concentration in gas condensate and weight of adsorbent due to their F-value, while the effect interaction variables are in the following order; time and concentration, volume, and concentration. The values of p are bigger

Table 2: Experimental factors and respective levels for optimization of sulfur removal from natural gas condensate using PAN/Ag fibers.

Variable	Factors	Level		
Adsorption time (min)	A	4	47	90
volume of sample (mL)	B	10	30	50
Initial sulfur concentration (mg/Lit)	C	100	450	800
adsorbent weight (mg)	D	10	20	30

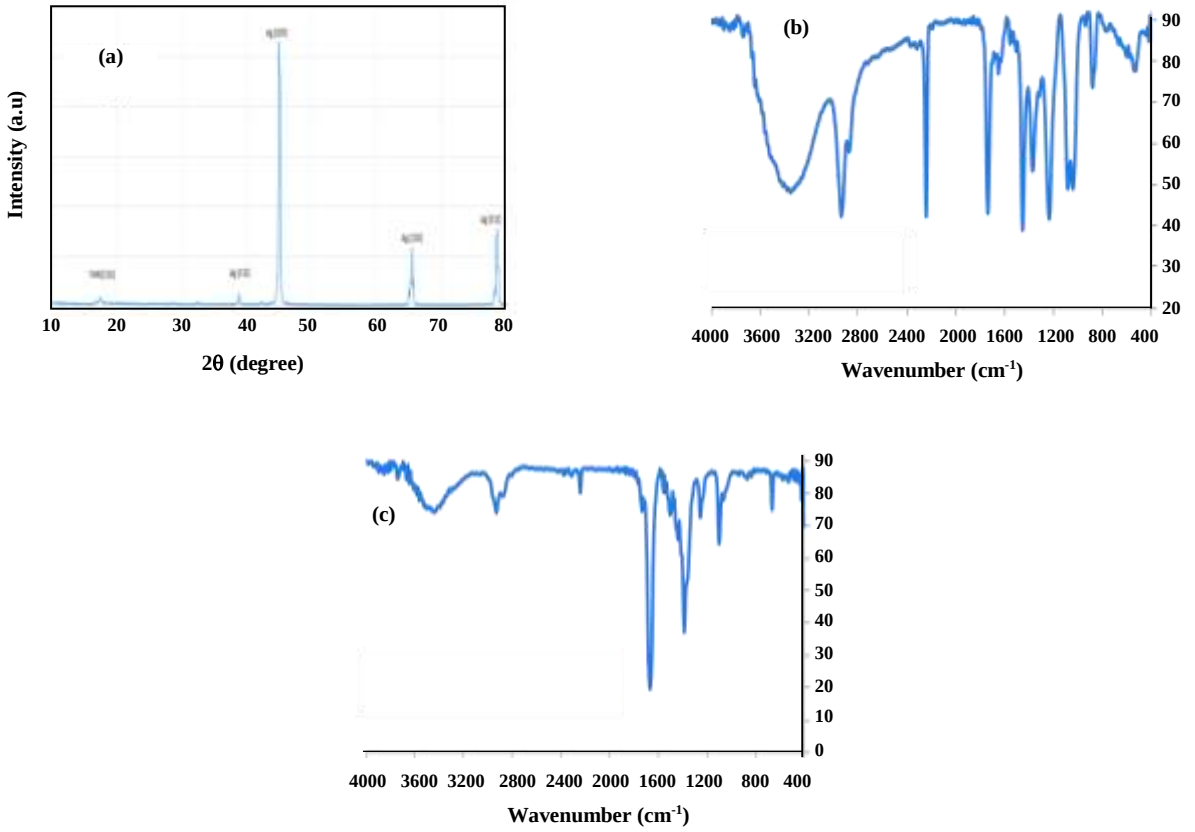

Fig. 3: (a) XRD pattern for PAN/Ag nanofiber, FT-IR spectra for (b) PAN nanofibers, and (c) PAN/Ag nanofibers.

than 0.05 indicate that the response does not affect by factor. The final equation model in terms of coded factors is:

$$R = +24.19 - 0.27A + 1.45B + 0.057C - 1.95D - 0.0018AB + 0.00036AC + 0.015AD - 0.00096BC - 0.049BD - 0.00046CD + 0.00057A^2 + 0.0076B^2 + 0.000018C^2 + 0.049D^2$$

The suggested second-order polynomial shows good convergence between actual and predicted results *via* its high correlation coefficient R^2, which indicated the assumed model is reasonably well fitted with actual data. The experimental results are very little diverging from the predicted results as illustrated graphically in Fig. 4a. Furthermore, the plot of the residuals versus the predicted values shows no distinct increasing or decreasing pattern (Fig. 4b) so the obtained model describes the experimental results well.

This polynomial model was used to construct the response surface to analyze the effect of the different variables on the adsorption capacity of the nanofibers.

Table 3: The conditions of each Run and the respective adsorption capacity values.

Run	Time (min)	Volume (mL)	Sulfur concentration (mg/Lit)	Adsorbent weight (mg)	Adsorption capacity (mg S/g adsorbent)
1	47	30	450	20	46.8
2	4	30	450	20	36.5
3	4	10	800	10	66.2
4	47	50	450	20	56.5
5	4	50	800	30	36.6
6	47	30	100	20	29.2
7	90	50	800	10	102.5
8	90	50	100	10	65.5
9	47	10	450	20	40.5
10	4	50	100	30	27.8
11	47	30	450	10	60
12	47	30	450	20	46.2
13	90	30	450	20	54.5
14	47	30	450	20	43.5
15	47	30	450	20	45.8
16	47	30	450	30	40.8
17	4	10	100	10	24
18	90	10	800	30	93.5
19	90	10	100	30	36
20	47	30	800	20	66
21	47	30	450	20	43.8

Table 4: The ANOVA results for the response surface quadratic model.

Source	SS	D_f	MS	F value	P value
Model	7958.26	14	568.45	378.35	<0.0001
A-time	128.00	1	128.00	85.19	<0.0001
B-volume	128.00	1	128.00	85.19	<0.0001
C-concentration	3323.33	1	3323.33	2211.94	<0.0001
D-weight	184.32	1	184.32	122.68	<0.0001
AB	3.91	1	3.91	2.60	0.1580
AC	236.53	1	236.53	157.43	<0.0001
AD	65.79	1	65.79	43.79	0.0006
BC	363.15	1	363.15	241.71	<0.0001
BD	155.63	1	155.63	103.58	<0.0001
CD	20.80	1	20.80	13.84	0.0098
A^2	2.80	1	2.80	1.87	0.2209
B^2	23.72	1	23.72	15.79	0.0073
C^2	11.78	1	11.78	7.84	0.0312
D^2	62.50	1	62.50	41.60	0.0007
Residual	9.01	6	1.50	_	_
Lack of fit	0.25	2	0.12	0.056	0.9460
Pure Error	8.77	4	2.19	_	_
Total	7967.28	20	_	_	_

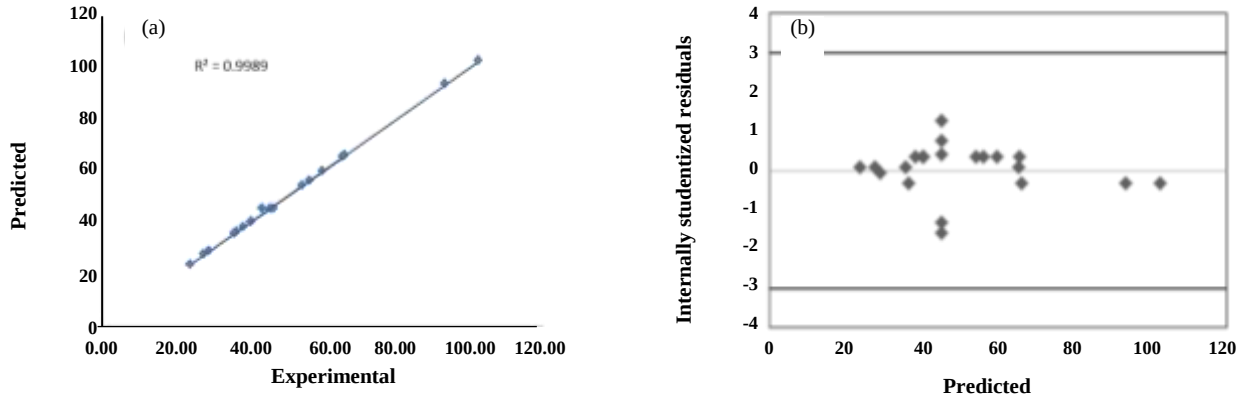

Fig. 4: (a) The predicted vs experimental values, (b) the residuals vs predicted values obtained from RSM model.

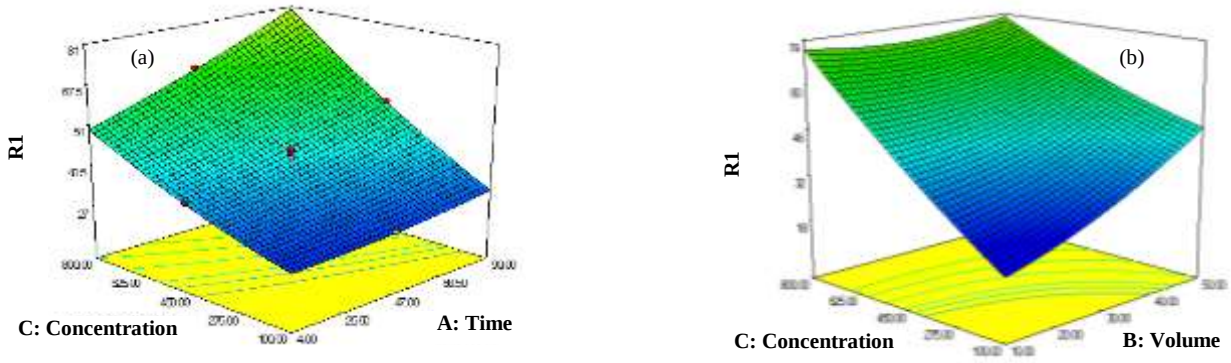

Fig. 5: 3D response surfaces of the adsorption capacity for (a) the adsorption time versus concentration at a volume of 30 mL gas condensate and weight of 20 mg nanofiber, (b) the sample volume versus its concentration at an absorbate weight of 20 mg and adsorption time of 47 min.

The relationship between the adsorption time and the sulfur concentration in the specimen, Figure 5a, shows that an increase in adsorption capacity is accomplished by a combination of high adsorption time and the concentration of sulfur compounds, meaning a good performance of adsorbent even at high concentrations of sulfur. The time-dependent nature of desulfurization by the developed nanofiber in this work implies its adsorptive nature of desulfurization. Based on Fig 5b, a gradual increase in adsorption capacity is also seen for an increase in the volume of specimen in the same concentration so that at the high concentrations and high volumes of the specimen, due to saturation of the surface of the adsorbent, the adsorption capacity reaches a plateau value.

Due to the considerable performance of this nanofiber along with its network structure, the membrane-based removal of sulfur compounds from natural gas condensate via optimized PAN/Ag nanofiber is under investigation in our laboratory.

CONCLUSIONS

In summary, considering the adsorption capacity of sulfur compounds from natural gas condensate as an objective function, the optimization of synthesis conditions of PAN/Ag nanofiber composites was first performed in this work via Taguchi experimental design. The PAN/Ag nanofibers with 11 wt% PAN, 45 wt% $AgNO_3$, 15 kV applied voltage, and 15 cm for a distance of needle to collector showed the highest adsorption capacity. In the second part of this work, the characterization of the optimized PAN/Ag nanofiber structure was elucidated by SEM, EDX, TEM, XRD, and FT-IR techniques. The characterization techniques affirmed the successful synthesis of PAN/Ag nanofibers with diameters in

100-300 nm range, with perfect distribution of Ag nanoparticles in a polymeric matrix. Moreover, the reduction nature of DMF as solvent and reductant was clarified from the comparison of the FT-IR spectrum of PAN and PAN/Ag. In the third part of this work, optimization of the adsorption capacity of PAN/Ag nanofiber in desulfurization of natural gas condensate in batch mode was performed *via* a central composite face center design. Four factors including adsorbent weight, sulfur concentration, the volume of sample, and adsorption time were considered effective factors each in three levels. The ANOVA analysis showed the more important factors that affected the adsorbent performance are the concentration of sulfur in gas condensate and the weight of the adsorbent. The interaction terms between time and concentration and between volume and concentration are also important in response. Moreover, the obtained polynomial model had the potential for prediction. The response surface analysis of interaction terms showed the adsorptive nature of desulfurization.

Acknowledgment

This work is supported by the South Pars Gas Complex and we gratefully acknowledge the SPGC due to the offering of laboratory facilities.

Received : Mar. 11, 2021 ; Accepted : Jun. 11, 2021

REFERENCES

[1] Song C., Ma X., New Design Approaches to Ultra-Clean Diesel Fuels by Deep Desulfurization and Deep Dearomatization, *Appl. Catal. B Environ*., **41**: 207–238 (2003).

[2] Javadli R., de Klerk A., Desulfurization of Heavy Oil, *Appl. Petrochemical Res.*, **1**: 3–19 (2012).

[3] Wang L., Yang R.T., New Nanostructured Sorbents for Desulfurization of Natural Gas, *Front. Chem. Sci. Eng.*, **8**: 8–19 (2014).

[4] Domańska U., Walczak K., Królikowski M., Extraction Desulfurization Process of Fuels with Ionic Liquids, *J. Chem. Thermodyn.*, **77**: 40–45 (2014).

[5] Moradi G.R., Rafiee E., Sahraei S., Jabari A., Deep Oxidative Desulfurization of Thiophenic Model Oil/Natural Gas Condensate over Tungsten/Molybdenum Oxides Using H_2O_2 as Oxidant, *Zeitschrift Für Anorg. Und Allg. Chemie.*, **642**: 566–571(2016).

[6] Monticello D.J., Biodesulfurization and the Upgrading of Petroleum Distillates, *Curr. Opin. Biotechnol.*, **11**: 540–546 (2000).

[7] Syed M., Soreanu G., Falletta P., Béland M., "Removal of Hydrogen Sulfide from Gas Streams Using Biological Processes - A Review", Can. Biosyst. Eng. / Le Genie Des Biosyst. Au Canada. 48 (2006).

[8] Khadir A., Mollahosseini A., Tehrani R.M.A., Negarestani M., A Review on Pharmaceutical Removal from Aquatic Media by Adsorption: Understanding the Influential Parameters and Novel Adsorbents BT - Sustainable Green Chemical Processes and Their Allied Applications, in: "Inamuddin", A. Asiri (eds.), Springer International Publishing, Cham, 207–265 (2020).

[9] Khadir A., Negarestani M., Mollahosseini A., Sequestration of a Non-Steroidal Anti-Inflammatory Drug from Aquatic Media by Lignocellulosic Material (Luffa Cylindrica) Reinforced with Polypyrrole: Study of Parameters, Kinetics, and Equilibrium, *J. Environ. Chem. Eng.*, 103734 (2020).

[10] Khadir A., Motamedi M., Pakzad E., Sillanpää M., Mahajan S., The Prospective Utilization of Luffa Fibres as a Lignocellulosic Bio-Material for Environmental Remediation of Aqueous Media: A Review, *J. Environ. Chem. Eng.*, 104691 (2020).

[11] Piri F., Mollahosseini A., Khadir A., Milani Hosseini M, Enhanced Adsorption of Dyes on Microwave-Assisted Synthesized Magnetic Zeolite-Hydroxyapatite Nanocomposite, *J. Environ. Chem. Eng.*, **7**: 103338 (2019).

[12] Khadir A., Motamedi M., Negarestani M., Sillanpää M., Sasani M., Preparation of a Nano Bio-Composite Based on Cellulosic Biomass and Conducting Polymeric Nanoparticles for Ibuprofen Removal: Kinetics, Isotherms, and Energy Site Distribution, *Int. J. Biol. Macromol.*, **162**: 663-677 (2020).

[13] Mollahosseini A., Khadir A., Saeidian J., Core–Shell Polypyrrole/Fe_3O_4 Nanocomposite as Sorbent for Magnetic Dispersive Solid-Phase Extraction of Al^{+3} Ions from Solutions: Investigation of the Operational Parameters, *J. Water Process Eng.*, **29**: 100795 (2019).

[14] Khadir A., Negarestani M., Ghiasinejad H., Low-Cost Sisal Fibers/Polypyrrole/Polyaniline Biosorbent for Sequestration of Reactive Orange 5 from Aqueous Solutions, *J. Environ. Chem. Eng.*, **8**: 103956 (2020).

[15] Mirjavadi E.S., Tehrani R. M.A., Khadir A., Effective Adsorption of Zinc on Magnetic Nanocomposite of Fe_3O_4/Zeolite/Cellulose Nanofibers: Kinetic, Equilibrium, and Thermodynamic Study, *Environ. Sci. Pollut. Res.* (2019).

[16] R.T. Yang, A.J. Hernández-Maldonado, F.H. Yang, Desulfurization of Transportation Fuels with Zeolites under Ambient Conditions, *Science* (80-.). 301: 79–81 (2003).

[17] Hernández- Maldonado A.J., Yang R.T., New Sorbents for Desulfurization of Diesel Fuels *via* π- Complexation, *AIChE J.*, **50**: 791–801 (2004).

[18] Bakhtiari G., Abdouss M., Bazmi M., Royaee S.J., Optimization of Sulfur Adsorption over Ag-Zeolite Nanoadsorbent by Experimental Design Method, *Int. J. Environ. Sci. Technol.*, **13**: 803–812 (2016).

[19] Tang X., Hu T., Li J., Wang F., Qing D., Deep Desulfurization of Condensate Gasoline by Electrochemical Oxidation and Solvent Extraction, *RSC Adv.*, **5**: 53455–53461 (2015).

[20] Gano Z.S., Mjalli F.S., Al-Wahaibi T., Al-Wahaibi Y., AlNashef I.M., Extractive Desulfurization of Liquid Fuel with FeCl3-Based Deep Eutectic Solvents: Experimental Design and Optimization by Central-Composite Design, *Chem. Eng. Process. Process Intensif.*, **93**: 10–20 (2015).

[21] Crespo D., Qi G., Wang Y., Yang F.H., Yang R.T., Superior Sorbent for Natural Gas Desulfurization, *Ind. Eng. Chem. Res.*, **47**: 1238–1244 (2008).

[22] Behl M., Yeom J., Lineberry Q., Jain P.K., Shannon M.A., A Regenerable Oxide-Based H_2S Adsorbent with Nanofibrous Morphology, *Nat. Nanotechnol.*, **7**: 810–815 (2012).

[23] Li C.-J., Li Y.-J., Wang J.-N., Zhao L., Cheng J., Ag+-Loaded Polystyrene Nanofibrous Membranes Preparation and Their Adsorption Properties for Thiophene, *Chem. Eng. J.*, **222**: 419–425 (2013).

[24] Huang Z.-M., Zhang Y.-Z., Kotaki M., Ramakrishna S., A Review on Polymer Nanofibers by Electrospinning and their Applications in Nanocomposites, *Compos. Sci. Technol.*, **63**: 2223–2253 (2003).

[25] Allafchian A.R., Gholamian M., Mohammadi J., Desulfurization of Gasoline Using Acrylonitrile Electrospun Nanofibers and Lead Nanoparticles, *Int. J. Environ. Sci. Technol.*, **14**: 1489-1496 (2017).

[26] Deitzel J.M., Kleinmeyer J., Harris D., Beck Tan N.C., The Effect of Processing Variables on the Morphology of Electrospun Nanofibers and Textiles, *Polymer (Guildf).*, **42**: 261–272 (2001).

[27] Pastoriza-Santos I., Liz-Marzán L.M., Formation and Stabilization of Silver Nanoparticles through Reduction by N,N-Dimethylformamide, *Langmuir*, **15**: 948–951 (1999).

[28] Wang Y., Yang Q., Shan G., Wang C., Du J., Wang S., Li Y., Chen X., Jing X., Wei Y., Preparation of silver Nanoparticles Dispersed In Polyacrylonitrile Nanofiber Film Spun by Electrospinning, *Mater. Lett.*, **59**: 3046–3049 (2005).

[29] Pastoriza-Santos I., Liz-Marzán L.M., N,N-Dimethylformamide as a Reaction Medium for Metal Nanoparticle Synthesis, *Adv. Funct. Mater.*, **19**: 679–688 (2009).

[30] Liu H., Ge, X. Ni Y., Ye Q., Zhang Z., Synthesis and Characterization of Polyacrylonitrile–Silver Nanocomposites by γ-Irradiation, *Radiat. Phys. Chem.*, **61**: 89-91 (2001).